UWB Channel Impulse Response Characterization Using Deconvolution Techniques

A. Muqaibel, **, A. Safaai-Jazi*, B. Woerner**, S. Riad**

*Time Domain and RF Measurement Laboratory
412 Whittemore Hall

**Mobile and Portable Radio Research Group (MPRG)
432 Durham Hall, Mail Stop 0350

The Bradley Department of Electrical and Computer Engineering
Virginia Polytechnic Institute and State University
Blacksburg, VA 24061-0111, USA

ABSTRACT

UWB Channels can be measured by sounding the channel with pulses, and thereby obtain the impulse response. Multipath components have different waveforms depending on the type of transmitter and receiver antennas used and the angles of transmission and reception. A modified deconvolution technique is introduced to extract the UWB channel response. The application of deconvolution techniques results in resolving multipath components with waveforms different from that of the sounding pulse. Resolving more components should improve the design of the rake receiver. Accurate characterization for the impulse response of a UWB communication system facilitates performance evaluation studies such as simulating the effect of pulse shaping.

1. INTRODUCTION

The importance of accurate channel characterization cannot be underestimated. There has been an appreciable amount of work to characterize the indoor propagation channel [1]-[3]. Ultra Wideband (UWB) impulse radio proposed in [4] has a promising future. With few exceptions including [5] and [11], most of the characterization measurements have been performed for narrow bands .

Before UWB impulse radio can be implemented for indoor applications, the UWB indoor channel need to be characterized. The early measurement attempts reported in the literature extend the narrowband measurement scenarios to the UWB case. Both the approach and the results need to be verified.

For narrowband characterization, usually no deconvolution is needed and the excitation signal is assumed to be close to an ideal Dirac-delta impulse which means that the received signal can approximate the impulse response. For narrowband channels, deconvolution was only used when super-resolutions were required [6]-[7]. Deconvolution is most needed for the characterization of wideband devices and channels due to the limited bandwidths of available test signals as compared to the bandwidths of devices and channels themselves [8]. Since the channel under study is wideband, deconvolution techniques are needed to estimate the UWB channel impulse response. Moreover, with deconvolution the estimated channel impulse response is independent of the excitation signal, which allows for the simulation of different waveforms for wave-shaping studies.

In the next section, we introduce the measurement system. In section 3, the deconvolution problem is formalized. The incentive for the proposed multi-template model deconvolution is given through experimental means. Improvements and results of applying the multi-template deconvolution algorithm are presented in section 4.

2. MEASUREMENT SETUP

An experimental setup was established in the Time Domain and RF Measurement Laboratory at Virginia Tech to evaluate the performance of an impulse radio. The setup consists of a pulse generator that sends impulses to a TEM horn transmitting antenna through a balun. The received signal is observed using a digitizing oscilloscope. The receiver antenna is also a TEM horn connected to the test set through a balun. The sampling oscilloscope is connected to a PC equipped with a data acquisition unit.

Synchronization is achieved through an external circuit. The sampling oscilloscope requires a pre-trigger. The oscilloscope has to receive the pre-trigger more than 80 nanoseconds before the trigger signal to the transmitter. This is achieved by using a step generator driver that can supply the required trigger and pre trigger signals.

Figure 1 shows both the transmitted pulse and the corresponding received pulse at a 2.5 meter distance required to confirm far field reception. The pulse has a slow falling edge which reduces the ringing effects and allows for easier time gating.

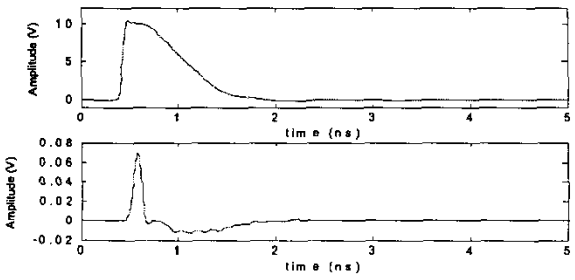

Figure 1. Transmitted and received pulses. The upper plot represents the transmitted pulse, while the lower plot represents the received pulse.

0-7803-7523-8/02/$17.00 ©2002 IEEE

A 50 *ns* representative received multipath profile in the line-of-site configuration is shown in Figure 2.

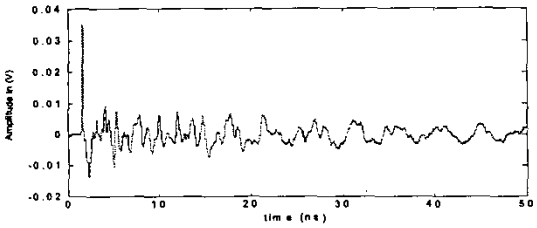

Figure 2. Typical received line-of-site multipath profile

3. DECONVOLUTION

Channels can be characterized by their transfer function in the frequency domain or by their impulse response in the time domain. The measurements under investigation were done in the time domain. Deconvolution of the time-domain waveforms can be used to determine the impulse response of a linear time-invariant system. The indoor channel is assumed to be time-invariant if the transmitter and the receiver are static and no motions take place in the channel.

If $h(t)$ is the impulse response of such a channel whose input is $x(t)$, then the output $y(t)$ is given by the convolution integral,

$$y(t) = x(t) * h(t) = \int_{-\infty}^{+\infty} x(\tau) \cdot h(t-\tau) d\tau \qquad (1)$$

where * denotes the convolution operation. In the frequency domain, convolution transforms into multiplication; that is,

$$Y(j\omega) = X(j\omega) \cdot H(j\omega) \qquad (2)$$

where $Y(j\omega)$, $X(j\omega)$ and $H(j\omega)$ are the frequency-domain representations of $y(t)$, $x(t)$, and $h(t)$, respectively.

The process of obtaining $h(t)$ knowing both $x(t)$ and $y(t)$ is called deconvolution. Ideally, deconvolution can also be performed in the frequency domain using the Fourier transform. Thus, from (2)

$$H(j\omega) = Y(j\omega) / X(j\omega). \qquad (3)$$

Due to measurement and signal processing limitations, simple division will result in noise-like error around the zeros of $X(j\omega)$. Filtering should be used to improve the estimation of the impulse response. A filter that demonstrated quality performance is given by the form [10]

$$H(j\omega) = 1 / \left[1 + \lambda / |X(j\omega)|^2\right] \cdot \frac{Y(j\omega)}{X(j\omega)} \qquad (4)$$

For the received profile, $y(t)$, shown in Figure 2 with $x(t)$ as the received line-of-site reference gated-pulse , the corresponding channel impulse response using (4) with $\lambda = 50$ is shown in Figure 3.. The impulse response, as shown in Figure 3, is not a summation of delayed delta functions. It is evident from the impulse response that multipath components have different waveforms compared with the reference pulse. Though, the transfer function and the impulse response give full channel description, only few parameters can be used by the receiver for channel estimation. Model deconvolution is usually used to characterize the channel with few parameters [9].

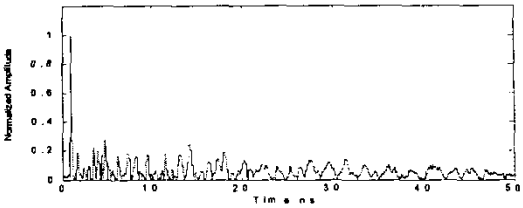

Figure 3. Typical line-of-site channel impulse response

3.1 Model (Subtractive) Deconvolution

The impulse response of the propagation channel is often modeled as a summation of effective scatterers,

$$h(t) = \sum_{i}^{I} a_i \delta(t - \tau_i) \qquad (5)$$

where a_i are the magnitudes of I scatterers. The model in (5) is widely used and can adequately represent the channel for many narrowband communications purposes. This model does not perfectly fit the UWB channel because the delta function at the receiver implies an infinite channel bandwidth, which is not possible or realizable. To make the model more accurate, the reference pulse used is the convolution of the sounding pulse, transmitter and receiver antennas, and the impulse response of the detector (sampling oscilloscope), Figure 4. This reference pulse is measured in a well behaved channel where the multipath reflections can be gated out. The transmitter and the receiver antennas are facing each other with a distance of 2.5*m* to guarantee far field reception for the antenna under use. Both the transmitted and received pulses are shown in Figure 1.

Though this technique is widely used, the assumption that the received pulses through different paths have the same waveform is not justified. This assumption requires that both the transmitter and the receiver antennas have spherical patterns at all frequencies. It was noted in [11] that if the antenna is electrically large compared to the wavelength of the center frequency of the received signal, the waveforms radiated in different directions

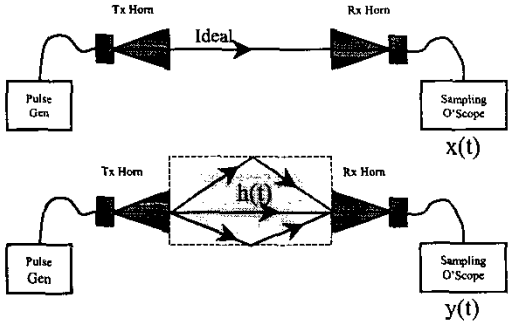

Figure 4. Illustration of the measurements of an ideal channel and a multipath indoor channel

from the transmitter antenna look considerably different in the far field region.

Here we also show that the waveforms received at different angles, look considerably different. Figure 5 illustrates a simple scenario where the transmitter and the receiver are facing each other and the receiver elevation angle is rotated in 15° steps.

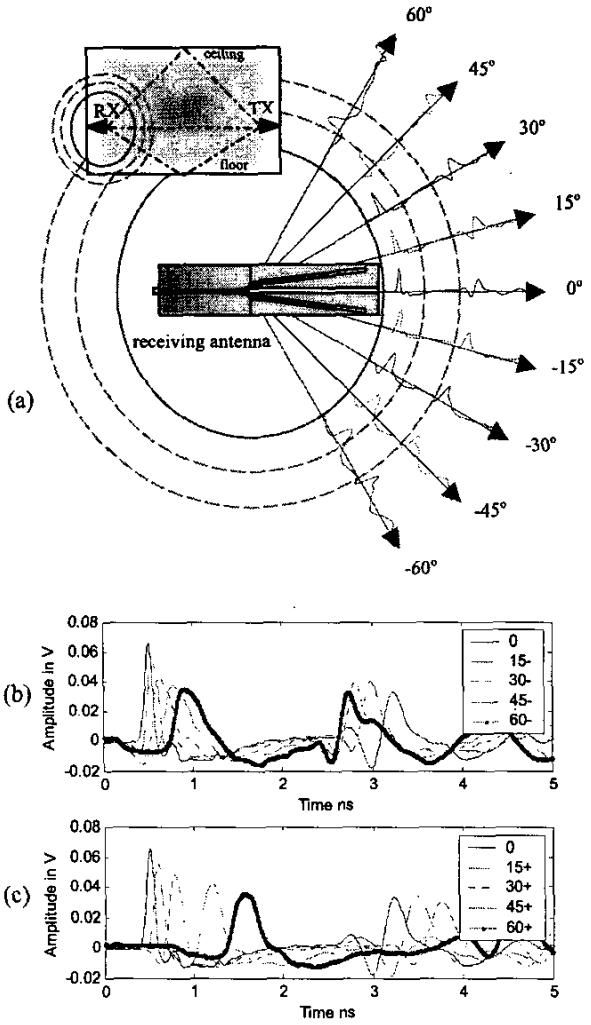

Figure 5: (a) Received waveforms at different receiver elevation angles. (b) and (c) the waveforms are redrawn for clarity and comparison.

Both the setup and the received waveforms are sown in Figure 5. Comparative plots are shown in Figures 5b and 5c. Both the line-of-site and the reflection from floor are shown in this figure.

Another illustrative experiment is performed with the two antennas directed towards a reflecting surface (floor). The setup for this experiment and the received waveforms are shown in Figure 6. For the setup shown in Figure 6, the waveform associated with the direct path is totally different from the reference waveform. On the other hand, the reflection from the floor, which has the same angle of arrival and transmission relative to the antennas, has the same shape as the reference waveform. The reference waveform is reproduced as an inset of the plot for comparison.

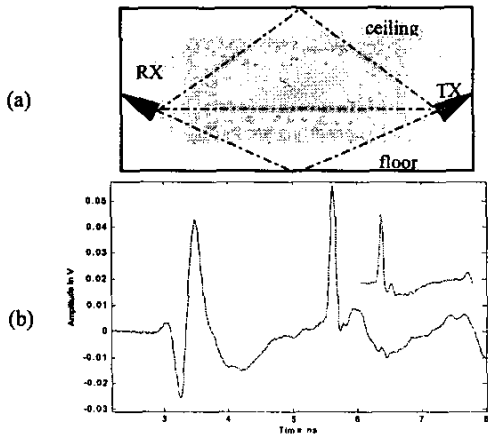

Figure 6. (a) Setup and (b) received waveform with both transmitter and receiver antennas pointing to the reflection surface.

3.2 Multi-Template Subtractive Deconvolution

Based on the previous experiments, it is evident that the assumption that multipath components have shapes similar to that of the reference line-of-site template is far from being valid. The same conclusion can be extended to other practical antennas. With this perception, the model can be modified to allow for more than one received pulse waveform. The model is antenna specific and is given by

$$h(t) = \sum_{j}^{J} a_j \tilde{h}^j (t - \tau_j) \qquad (6)$$

where $\tilde{h}^j$ is the impulse response of a system, which when excited by the line-of-site pulse $\tilde{p}^1$ the output is the jth template $\tilde{p}^j$. When the received signal is the line-of-site then it corresponds to $\tilde{h}^1 = \delta(t)$. Assuming k different templates, the subtractive deconvolution algorithm is modified from that described in [6] as follows:

1) initialize the dirty map with the received waveform $r(t)$ $d(t)=r(t)$ and the clean map with $c(t)=0$;
2) form the correlation coefficient functions $\Gamma^j(\tau) = \tilde{p}^j(t) \Theta d(t)$, (normalization is understood and Θ means correlation), for $j=1,2,...k$;
3) find the peaks (max $\Gamma_i^j, j=1,2,...k$), and their positions, τ_i, in the $\Gamma^j(\tau)$;
4) if all $\Gamma_i^j <$ threshold, go to step 8;
5) clean the dirty map by inserting zeros in place of the detected multipath component;

6) update the clean map by using $c(\tau) = c(\tau) + \Gamma_i^j h^j(t - \tau_i)$.

7) go to step 2;

8) the impulse response is then $\hat{h}(t) = c(t)$.

Note that in *step* (5) updating the dirty map is done by inserting zeros in place of the detected component rather than updating by replacing *d(t)* with $d(t) - \Gamma_i^j \tilde{p}^j(t - \tau_i)$ as in [6]. This inherently assumes that multipath components do not overlap. We justify this assumption because of the dispersive nature of the environment. If the dirty map is updated as in [6], invalid multipath components will be produced as a result around the previously detected components. As a result of zeroing the window of the detected component, not all the energy can be captured.

In the next section, the modified subtractive deconvolution is applied to the previous channel with different number of templates.

4. RESULTS AND ANALYSIS

The energy in the above multipath profile is now captured using a correlator with a fixed template and compared with that obtained using the proposed multi-template correlator. For the multi-template case, the reference templates are based on antenna measurements at different elevation angles.

Figure 7 shows the improvement in the captured energy versus the number of captured multipath components. Different traces are shown for different number of templates. For the case of single template, the reference template was measured at 0° in a well-behaved environment where reflections could be gated out. For the case of two templates, the reference templates were measured at 0° and 45°. For the case of three, four, and five reference templates, the measurements were performed at the following sets of elevation angles (0°, 45°, 60°), (0°, 30°, 45°, 60°), and (0°,15°,30°, 45°, 60°), respectively. The choices of templates were not fully optimized but rather were based on the shape of the reference waveform to allow capturing more energy.

Using two templates resulted in more than 10% increase in the captured energy. With 20 single-path correlators, the performance saturated with three templates at about 53% of the received energy. The limit in the maximum captured energy is a direct result of the assumption that multipath components are not allowed to overlap.

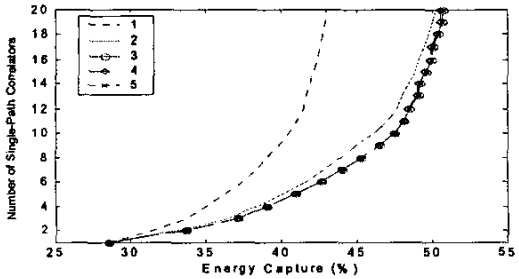

Figure 7. Improvement in captured energy versus number of single-path correlator for different number of reference templates.

5. SUMMARY AND CONCLUSIONS

In this paper, we presented some experimental results to illustrate that UWB multipath components my have dramatically different waveforms at different angles relative to the transmitter and receiver antennas. A multi-template UWB propagation model was proposed to account for the received components at different angles. Subtractive deconvolution was modified and used to extract the model parameters from measured channel profiles. The resultant impulse response is antenna-specific. It was shown that the captured energy increases by more than 10% when using two reference waveforms. Further extension of the work would include optimizing the choices of reference templates based on extensive antenna measurements and applying the modified multi-template model and deconvolution algorithm to extensive channel measurement campaign.

6. REFERENCES

[1] Hashemi H.,"The indoor radio propagation channel," *Proc. IEEE*, vol. 81, no. 7, July 1993.

[2] Hashemi H.,"Impulse Response Modeling of Indoor Propagation Channels," *IEEE Journal of Selected Areas in Communications*, vol. 11, No. 7, Sept. 1993.

[3] Rappaport T., "Characterization of UHF multipath radio channels in factory buildings," IEEE Transactions on Antennas and Propagation , vol. 37, no. 8 , pp. 1058 – 1069, Aug. 1989.

[4] Scholtz R.A., "Multiple access with time-hopping impulse modulation," MILCOM '93 Proceedings, vol. 2, pp. 447 – 450, 1993.

[5] Win M. and Scholtz R., "Energy Capture vs. Correlator Resources in Ultra-Wide Bandwidth Indoor Wireless Communications Channels," MILCOM '97 Proceedings, vol. 3 , 1997, pp. 1277-1281.

[6] Vaughan R. and Scott N., "Super-Resolution of Pulsed Multipath Channels for Delay Spread Characterization," *IEEE Transactions on Communications*, vol. 47, no.3, pp. 343-347, Mar. 1999.

[7] Morrison G. and Fattouche M., "Super-Resolution Modeling of the Indoor Radio Propagation Channel," *IEEE Transactions on Vehicular Technology*, vol. 47, no. 2, pp. 649-657, May 1998.

[8] Parruck B. and Riad S., "An Optimization Criterion for Iterative Deconvolution" IEEE Transaction on Instrumentation and Measurement, vol. IM-32, no.1, Mar. 1983.

[9] Norris N. S. and Guillaume M. "Deconvolution of Time Domain Waveforms in the Presence of Noise," National Bureau of Standards, 3

[10] Riad S., "The Deconvolution Problem: An Overview," *Proceedings of the IEEE*, vol. 74, no. 1, pp. 82-85, Jan. 1986.

[11] Cramer R., Scholtz R., and Win M. "Evaluation of an Ultra-wide-Band Propagation Channel," *IEEE Transactions on Antennas and Propagation*, vol. 50, no. 5, pp. 561-570, May 2002.